Processing and characterization of improved congruent lithium niobate

A. A. Anikiev,[1,a] M. F. Umarov,[2] and J. F. Scott[3]
[1]*Bauman State Technical University, 105005 Moscow, Russia*
[2]*Vologda State University, 160000 Vologda, Russia*
[3]*Schools of Chemistry and Physics, Univ. St. Andrews, St. Andrews KY16 9ST, United Kingdom*

(Received 7 September 2018; accepted 5 November 2018; published online 15 November 2018)

$LiNbO_3$ exists in two forms: Most commercial devices are inexpensively fabricated from congruent melt that is ca. 1.5% off-stoichiometry. This produces devices of high optical quality for nonlinear optics but also high loss. Stoichiometric lithium niobate also exists, but in smaller more expensive specimens. Here we report the preparation and characterization of low-loss congruent samples. These are shown to be relatively free from extended defects. https://doi.org/10.1063/1.5055386

For some years there was a controversy in $LiNbO_3$ and $LiTaO_3$ concerning their ferroelectric phase transition dynamics. Some researchers concluded that these were displacive phase transitions with soft optical phonons, whereas others argued that they were order-disorder. This disagreement arose primarily because the soft mode is heavily damped, and near the Curie temperature the spectra of the specimens therefore resemble that of disordered materials. However, this was misleading, in that almost all samples used in the early years (<1985) were non-stoichiometric, pulled from a congruent melt. Such specimens have aproximately 1.5% off-stoichiometric Li/Nb ratio, corresponding to an enormous defect concentration of ca. 10^{21} cm^{-3}, which will create a disordered Raman spectrum, independent of the intrinsic dynamics.

Following work[1,2] that included stoichiometric samples, experts in the field recognized that the intrinsic dynamics are primarily displacive, and that there are two qualitatively different kinds of spectra – congruent and stoichiometric.

It has generally been considered that the poorer optical and electrical properties in congruent specimens arise simply from the lack of stoichiometry; however, we dispel this myth by making measurements on a number of specimens with exactly the same stoichiometry (and hence the same number of point defects or vacancies) but different densities of extended defects. In the present work we update these studies of thirty years ago by showing that there are actually three kinds of $LiNbO_3$, not two: (1) Stoichiometric; (2) congruent with point defects; or (3) congruent with extended defects. We describe a processing technique that minimizes or eliminates the extended defects and thereby produces low-loss congruent samples that compete with stoichiometric ones but are commercially attractive because of larger size and lower cost; stoichiometric $LiNbO_3$ is available in several countries in sizes up to 2"-diameter wafers, whereas congruent samples can be readily purchased in 4" diameter wafers (e.g., Nano Co. in South Korea) and orders taken for 6" wafers (an increase by 900%).

Congruent lithium niobate is used commercially as periodically poled waveguides,[3] and this might benefit from lower-loss devices. Russia may be the largest producer of $LiNbO_3$ devices because it has 40 years use there for dual-use (commercial and military) equipment. However, suppliers in several countries (USA, UK, Sweden, China, Korea, Israel) often keep processing details proprietary; and it is generally not in accord with publication protocols to cite numbers from advertising material, as opposed to refereed journals with accessible raw data. Progress in the field of quasi-phase matching

[a]E-mail: aaanikyev@mail.ru

in nonlinear media and, in particular, in congruent lithium niobate crystals has been described in an excellent review by F. Laurell[4] and in a number of articles by this author.[5,6] Broad prospects for the commercial use of congruent lithium niobate as photonic and phonon crystals in devices of nonlinear optics and acousto-electronics are also well known after Gil Rosenman's work[7] on creating a regular submicro-domain structure in lithium niobate with the help of an atomic force microscope, and from the group of Pamela Thomas[8] on studying physical processes in the vicinity of domain wall boundaries using a high–resolution X-ray topography method. Extended defects in $LiNbO_3$ contribute to the well-studied problems of optical damage.[9,10]

EXPERIMENT

The congruent $LiNbO_3$ crystals studied in this paper were grown in the Scientific and Production Association PHONON facility in an air atmosphere from a melt of a congruent composition with uncontrolled impurities in the initial Li_2O-Nb_2O_5 burden by the Czochralski method. The growing conditions were changed to assess the influence of dislocations and other macrodefects on the quality of piezoresonators fabricated from lithium niobate: the rate of stretching of the seed from the melt varied in various experiments from 5 mm/hr to 23 mm/hr. In all experiments with different drawing speeds, the seeding rotation rate remained unchanged at 15 rpm. The axial gradient was 3^o – 5^o C/mm. It is known[11] that a decrease in the drawing speed leads to a sharp decrease in the dislocation density in lithium niobate crystals. At present, the growth of good quality lithium niobate crystals with a low concentration of intrinsic defects is carried out at crystal extraction rates from the melt not exceeding 0.1-0.3 mm/h and an axial gradient of not more than 1^oC/mm.

We have examined the quasi-elastic light scattering spectra in lithium niobate samples of various degrees of imperfection, determined from the acoustic quality factor at a temperature of 296 K. A quantitative analysis of the spectra was carried out in the frequency range 0 - 70 cm^{-1} for samples with different Q-factors, of a model that takes into account the coupling of the low-frequency optical mode of A_1(TO) symmetry with a relaxing self-energy describing stoichiometry defects. Comparing the model calculations with the experimental data allows us to conclude that the stoichiometry defects play an important role in the formation of the dynamic central peak in the structural phase transition in congruent lithium niobate crystals. Of more practical technology transfer importance, these improved congruent samples have low loss factors that rival more expensive, small stoichiometric specimens.

The Raman spectra of the initial samples with measured Q-factors (we will call them samples of type I), were compared with Raman spectra on samples of other origin grown under controlled impurity conditions (type II).

The stoichiometric and congruent $LiNbO_3$ single crystals (samples II) with controlled impurities were grown in the Institute of Chemistry, the Kola Science Center of the Russian Academy of Sciences also in an air atmosphere by the Czochralski method from the Li_2O-Nb_2O_5 melt with 58.6 mol. % Li_2O and a congruent melt, respectively. For the congruent melt, a granular mix of congruent composition (48.6 mol% Li_2O) was used, obtained by the synthesis-granulation method. In particular, analysis of the synthesis, purification and granulation processes of the initial charge allowed the authors[12–15] to conclude that the most progressive technology for obtaining a burden of congruent composition is synthesis and granulation carried out in a single technological process in the temperature range 1100 – 1250 °C excluding multiphase and providing a high bulk density. In this case, the industrial production of large-sized crystals becomes economically more profitable, since the cost of a mass unit of the finished product decreases. An obligatory condition for obtaining large-size crystals of high optical quality when grown under conditions of a small axial gradient is also the provision of a high symmetry of the thermal field at the crystallization front. For example, with a temperature gradient at the boundary of a melt-crystal of 1.4°C/mm, an isothermal zone of 1220 °C, a drawing speed of 1.2 mm/h and a rotation speed of 12 rpm, large crystals 80 mm in diameter and 120 mm in length were grown.[12] The mass of the boule was 2300 grams. The crystals participating in our experiments were grown with the following parameters: the concentration of cation impurities in the mix was controlled and did not exceed 5×10^{-4} wt. % level or less, the drawing speed was 1.1 mm/h; the rotation speed was 14 rpm. The axial gradient was 1^oC/mm.

Samples of type I for Raman spectroscopy experiments were excised from monodomainized crystals in the rectangular parallelepipeds measuring $9 \times 7 \times 5$ mm^3, whose edges coincided with the directions of X, Y, and Z crystallographic axes. The facets of the samples were polished.

Raman spectra were excited by a 514.5 nm line of an argon laser and recorded on a modernized DFS-24 double monochromator with a photon counting system. The power of the exciting radiation did not exceed 2 mW. The spectra were recorded at a resolution of 1-2 cm^{-1}. The spectra were processed using Origin Pro v. 8; the accuracy of determining the frequencies, widths, and line intensities was ± 2 cm^{-1}, ± 3 cm^{-1} and 6%, respectively.

Samples of type II for studying Raman spectra were cut from single-domain crystals in the form of rectangular parallelepipeds measuring $8 \times 7 \times 6$ mm^3, whose edges coincided with the directions of X, Y, and Z crystallographic axes. The faces of the samples were polished.

The Raman spectra were excited with a 514.5 nm line of the Spectra Physics argon laser (model 2018-RM) and recorded with a Horiba Jobin Yvon T64000 spectrograph using a confocal microscope. The spectra were processed using Horiba LabSpec 5.0 and Origin 8.1. The accuracy of determining the frequencies, widths and intensities of the lines was ± 1 cm^{-1}, ± 3 cm^{-1} and 5%, respectively.

Measurements of the acoustic Q-factor were performed on samples of lithium niobate type I with sections (Y + 36^o) by resonant radio engineering method at a frequency of 300 MHz. Only five samples were prepared, with different values of the measured Q-Factor.

The Raman spectra of one of the samples of congruent crystals of type I with the highest Q-Factor of Q = 1.45x10^4 recorded in scattering geometry X (ZZ) Y are shown in Fig. 1a. In this scattering geometry, there are 4 vibrations of A_1 (TO) - symmetry. As can be seen from the figure

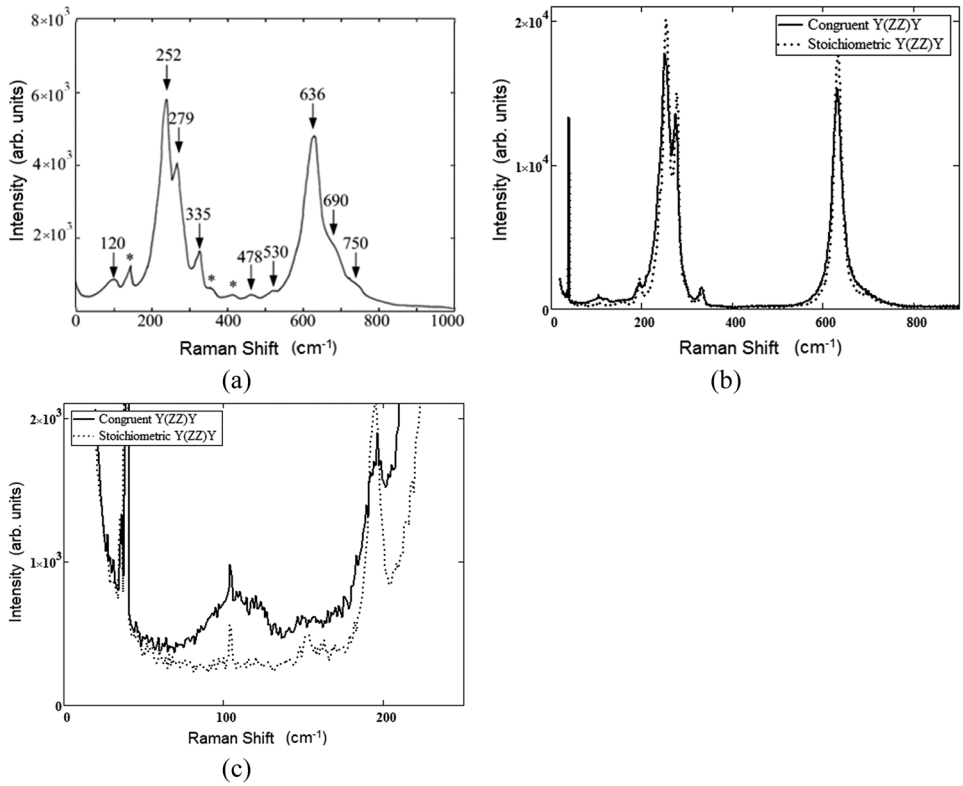

FIG. 1. a) Raman spectra of a congruent lithium niobate crystal of type I at a temperature T = 294K for the polarization geometry X(ZZ)Y. Peaks marked with an asterisk correspond to fundamental vibrations of the E(TO) symmetry. b) Raman spectra of congruent (solid line) and stoichiometric (dashed line) samples of lithium niobate type II for polarization geometry $Y(ZZ)\bar{Y}$ at temperature T = 296K in the frequency range 5- 800 cm^{-1}. c) The same Raman spectra in the low-frequency region 5-250 cm^{-1} in a 4:1 scale in comparison with spectra B).

in the spectrum, along with four modes of the A1 (TO) -type symmetry, the E (TO + LO) -type symmetry modes also appear. Moreover, additional features are observed in the spectrum: a wide band in the frequency range of 120 $cm^{-1}$and bands at 690 and 750 cm^{-1}, which do not belong to the fundamental vibrations of the structure of lithium niobate.

As a comparison, in Figs. 1b and 1c Raman spectra of congruent and stoichiometric crystals of lithium niobate type II, grown from a purified mix with controlled impurities, are shown in the scattering geometry Y(ZZ)Y.

The experimental data show that there is a significant difference in the widths of the fundamental lines for type I and II crystals, which results from the different loading used in the growth process. This parameter indicates the degree of imperfection or the degree of defectiveness of the samples. Furthermore, a large number of additional lines observed in the Raman spectra of type I samples also implies a considerable degree of disorder in the crystal structure. The 152 cm^{-1}, 369 cm^{-1}, and 432 cm^{-1} peaks marked with an asterisk in Fig. 1a correspond to fundamental vibrations of the E(TO) symmetry that appear in this scattering geometry due to a small misalignment in the orientation of the crystal or the orientation of the polarizer relative to the ideal arrangement of the X, Y, Z axes as well as an increase in the depolarization of scattered light as a result of structural imperfections.

In addition, in the spectrum in Figure 1 lines with frequencies of 120, 478, 530, 690 and 750 cm^{-1} are detected that are not related to the fundamental vibrations of any allowed type of symmetry. Calculations from the first principles of the dynamics of lattice vibrations of lithium niobate performed in Refs. 16–18 also do not confirm the fundamental vibrations close to the indicated frequencies, both resolved in Raman spectra and forbidden types of symmetry, including A_2 - symmetry vibrations. A comparison of Figures 1a and 1b shows that in congruent crystals of both types there is a broad band in the frequency range 100-120 cm^{-1}, which is not detected in stoichiometric samples of type II (Fig. 1c). Measurement of low-frequency Raman spectra in the temperature range 100K-440K does not reveal an increase in the intensity of the band at a frequency of 120 cm^{-1}, which is specific for second-order spectra.[19,20] At the same time, when the congruent samples are heated from 400 K to 1200 K, an appreciable shift and anomalous broadening of the 274 cm^{-1} low-frequency mode passing through the 254 cm^{-1} mode is observed.[1] The band in the 120 cm^{-1} frequency region increases strongly in intensity and merges with the wing of the quasi-elastic scattering line, the intensity of which also sharply increases. One generally assumes that the origin of the band in the frequency region of 120 cm^{-1} in congruent samples is related to the one-phonon density of acoustic states, which appears in Raman spectra. This band is manifested due to violation of the selection rules for the wave vector

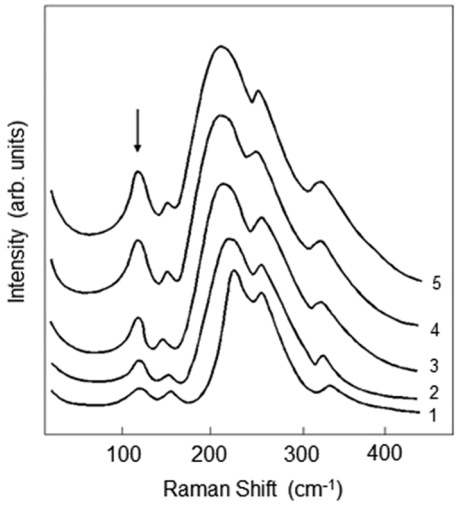

FIG. 2. Low-frequency Raman spectra of A_1 (TO) phonons obtained in X (ZZ) Y scattering geometries for samples of lithium niobate with various acoustic Q-factors: 1) Q = 1.45 x 10^4; 2) Q = 1.17 x 10^4; 3) Q = 0.85 x 10^4; 4) Q = 0.52 x 10^4; 5) Q = 0.35 x 10^4. Black arrow shows the band 120 cm^{-1} position in samples of lithium niobate with different Q-factors.

conservation, due to defects. This assumption is supported by the fact that the spectral shape of this band changes in different scattering geometries.

Figure 2 shows the low-frequency Raman spectra of lithium niobate samples of type I with different acoustic Q-factors recorded in the scattering geometry X (ZZ) Y corresponding to A_1 (TO) -type symmetry.

As can be seen in the figure, the intensity of the band in the frequency region of 120 cm^{-1} increases significantly with decreasing Q-factor from 1.45 x 10^4 to 0.35 x 10^4.

ANALYSIS

The increase in the intensity of the 120 cm^{-1} band correlates with the broadening of fundamental vibration lines of 1A(TO) and 2A(TO). There is a direct relationship between the intensity of the band under discussion and the acoustic quality factor: with decreasing Q-factor (increasing acoustic absorption), the intensity of the band increases according to a logarithmic law.

Spectral intensity of the 120 cm^{-1} band can be approximated by a linear law of the form

$$I(Q) = a \cdot Log(Q) + b, \tag{1}$$

where a = -0.99 ± 0.07 and b = 4.25 ± 0.27. The goodness of the approximation is 0.98. Figure 3 shows the spectral intensity of the 120 cm^{-1} band that depends on the quality of the samples.

It must be noted that a significant correlation between the intensity of the line at a frequency of 120 cm^{-1} in the Raman spectra of low frequencies and the molar composition of the K_2O flux in the initial mix was observed while studying various methods of growing nominally pure lithium niobate crystals.[14,15]

The results of this paper show that firstly the line under discussion can indeed be an important quantitative sign of the defectiveness of the structure of lithium niobate. Secondly, a high degree of correlation between the line intensity and the acoustic quality of the samples indicates the origin of the band as a singularity of the density of acoustic states, manifested in the first-order spectrum as a result of violation of the selection rules for the wave vector in the ever increasing region of the Brillouin zone due to an increase the dislocation density and increase the distortion of the ideal lattice.

Generally speaking, lithium niobate belongs to non-stoichiometric phases of variable composition, and such crystalline structures, as a rule, have a high degree of defectiveness, stoichiometry defects, structural and concentration heterogeneity in composition. Moreover, as recent studies conducted by the P. Thomas group[21,22] on crystals of lead zirconate titanate solid solutions have shown,

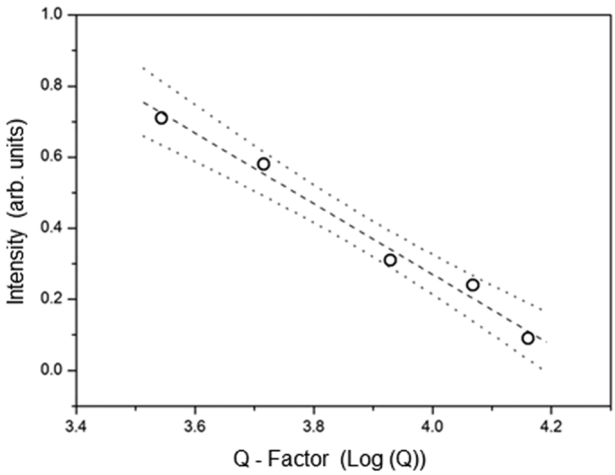

FIG. 3. The intensity of the 120 cm^{-1} band in type I lithium niobate samples depending on the acoustic Q-factor in logarithmic scale. The dashed line shows the approximation of empirical data (circles) by a linear law. The dotted lines represent the confidence zone with 95% probability.

the origin of high piezoelectric effect values is associated with the coexistence of monoclinic and rhombohedral phases. The discovery made by this group represents a new approach to interpreting of the properties and vibrational spectra of oxygen ferroelectrics having phases of variable composition. All these defects, both point defects and macroscopic defects, including a phase boundary, make also a significant contribution to the Rayleigh quasielastic and elastic scattering of light.

In this regard, along with the features of low-frequency Raman spectra, we have studied the relationship between the intensity of quasi-elastic light scattering and the defectiveness of samples. . In order to do that we plotted the scattering of light at frequencies of 70, 50, 40, 30, 20, and 10 cm^{-1} for samples with different Q-factors in Fig. 4. All spectra were normalized to the level of the exciting line.

These empirical data can best be described by an exponential law of the form:

$$I(Q) = I_0 + A \cdot exp(-B \cdot Q) \tag{2}$$

Fitting the data gives values of the optical phonon damping, the interaction constants and the relaxation time:

$$\gamma(0) = 562\ cm^{-1},\ \delta(0) = 227\ cm^{-1} \text{ and } \tau(0) = 1.42\ ps.$$

The intensity of the central peak (quasi-elastic scattering at zero frequency) depends on the quality factor of the samples and can be approximated by a power law:

$$\begin{aligned} &I(\omega = 0, Q) = A_0 + B_0 \cdot Q^{C_0} \\ &\text{Here } A_0 = -0.56,\ B_0 = 1.0,\ C_0 = -1.0.' \end{aligned} \tag{3}$$

Thus, the intensity of the quasi-elastic scattering at zero frequency diverges as Q tends to zero (the increase of sound absorption coefficients) with the power $\beta \approx -1.0$. This result is consistent with the conclusion of Ref. 23, which shows that the intensity of the quasi-elastic scattering should increase proportionally the concentration of defects.

The parameters of optical phonon "linewidth", coupling constant and relaxation time increase exponentially with a reduction of acoustic quality factor (increase in the density of dislocations) in the samples. A correlation submatrix for these parameters γ, δ and τ is shown in Table I.

Elastic scattering intensity at zero frequency diverges according to a power law with a power close to unity, as Q decreases to zero (increase in the dislocation density). Obviously, the intensity of elastic scattering in our experiment is proportional to the concentration of dislocations. Nevertheless, the particular form of relation between sound absorption coefficient and concentration of the dislocations is unknown. That is why in order to quantify the dislocation density and establish the relationship between dislocation density and coefficient of sound absorption we need to conduct the experiment of

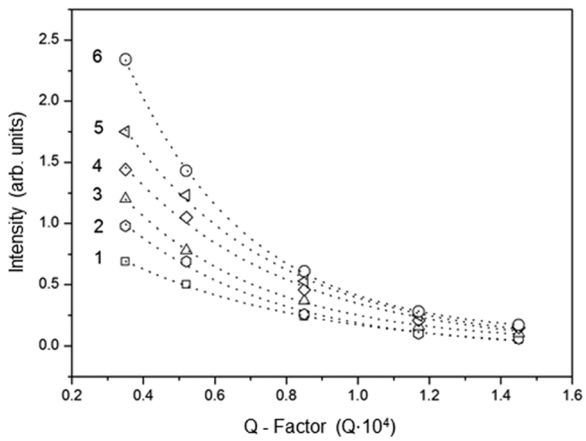

FIG. 4. The intensity of light scattering depending on the Q-factor in congruent lithium niobate samples at different frequencies: 1) 70 cm^{-1}; 2) 50 cm^{-1}; 3) 40 cm^{-1}; 4) 30 cm^{-1}; 5) 20 cm^{-1}; 6) 10 cm^{-1}. Dotted lines show the results of fit to (2).

TABLE I. Representative correlation submatrices for the approximation parameters of congruent lithium niobate samples light scattering spectra.

	Congruent specimen at Q1 = 1.45×10^4		
	γ, cm^{-1}	τ, s	δ, cm^{-1}
γ, cm^{-1}	1.00	0.93	-0,987
τ, s	0.93	1.00	-0.96
δ, cm^{-1}	-0.987	-0.96	1.00
	Congruent specimen at Q5 = 0.35×10^4		
γ, cm^{-1}	1.00	0.89	-0.966
τ, s	0.89	1.00	-0.94
δ, cm^{-1}	-0.966	-0.94	1.00

X-ray topography for each participating in the experiment samples. And although the mechanisms of elastic static and dynamic light scattering were mainly discussed in connection with the observation of the central peak in the vicinity of phase transitions, i.e. near the lattice instability, such conditions can be prepared by creating various concentrations of large-scale defects in the process of growing crystals. Thus, the lattice instability is modeled to some extent with respect to defects and it becomes possible to quantitatively estimate the contribution of defects to the quasi-elastic and elastic scattering parameters of light.

SUMMARY

The spectra of quasi-elastic light scattering in congruent lithium niobate crystals with extended defects are investigated. The experiments were carried out on samples grown at different drawing speeds; the stresses arising in the samples under such conditions led to the formation of dislocations with a density proportional to the rate of stretching of the seed. The degree of defectiveness of the samples was estimated from the acoustic quality factor, measured by the resonant radio engineering method. The increase in defect concentration led to significant broadening of the low-frequency optical modes of A_1(TO) symmetry with a simultaneous increase in the intensity of quasi-elastic scattering on the wing of the Rayleigh line. The behavior of the Rayleigh scattering intensity on defects is well described in the interaction model of a quasi-harmonic oscillator with damping and slow motions of acoustic modes on defects with a characteristic relaxation time τ (C), where C is the concentration of dislocations. The coupling strength between the optical mode and the relaxation of acoustic phonons on defects δ^2(C) depends on the concentration of defects, and the connection between these excitations occurs through damping. The good agreement of the experiment with the using model gave an opportunity to estimate the nature of the dependence of the damping of the optical phonon, the strength of the bond and the relaxation time on the defect concentration: these quantities increase exponentially with decreasing acoustic quality factor (an increase in dislocation density) in the samples.

The spectral intensity of quasielastic scattering at low frequencies normalized to the Bose factor shows a quadratic dependence on the frequency: in the logarithmic scale at 10-40 cm^{-1} frequencies, the reduced spectral intensity depends quadratically on the frequency with the power ν^{α}, $\alpha \approx 2.1$. This fact confirms the relaxation mechanism Rayleigh scattering of light by defects.[24] At the same time, the intensity of elastic scattering at zero frequency, obtained by the approximation of the model used, diverges with an unlimited increase in the defect concentration in accordance with the power law with linear index $\beta \approx 1.02$. The results of the work may have some interest in estimating the contribution of defects to the intensity of light scattering in the vicinity of structural phase transitions, since the lattice instability can be obtained not only by external effects on the crystal, but also by growth conditions of crystals with a controlled defect concentration. Likewise, the sensitivity of the band intensity in the region of 120 cm^{-1} and the quasi-elastic scattering of light from the defect concentration can be quantitative indicators of the degree of structural imperfections. Moreover, the construction of a calibration curve for the determination of the quality factor at room temperature from the light

scattering spectra can be carried out in two ways: from the intensity of the scattering of the resonance line of acoustic phonons at 120 cm^{-1} peak frequency in accordance with (1) and in the intensity of quasi-elastic scattering at low frequencies from (2). Thus, the results obtained make it possible to estimate from Raman spectra the density of extended defects in this improved low-loss kind of congruent lithium niobate crystals.

ACKNOWLEDGMENTS

The authors are grateful to Nikolai Sidorov of the Institute of Chemistry for useful discussions about the methods of growing lithium niobate crystals with controlled impurities and structural defects.

[1] Y. Okamoto, P.-c. Wang, and J. F. Scott, Phys. Rev. B **32**, 6787 (1985).
[2] M.-s. Zhang and J. F. Scott, Phys. Rev. B **34**, 1880 (1986).
[3] M. Yamada, N. Nada, M. Saitoh, and K. Watanabe, Appl. Phys. Lett. **62**, 435 (1993).
[4] V. Pasiskevicius, G. Strömqvist, F. Laurell, and C. Canalias, Optical Materials **34**(3), 513 (2012).
[5] M. Manzo, F. Laurell, V. Pasiskevicius, and K. Gallo, Appl. Phys. Lett. **98**(12), 122910 (2011).
[6] M. Henriksson, L. Sjöqvist, V. Pasiskevicius, and F. Laurell, Applied Physics B **86**(3), 497 (2007).
[7] G. Rosenman, P. Urenski, A. Agronin, and Y. Rosenwaks, Appl. Phys. Lett. **82**, 103 (2003).
[8] Z. W. Hu, J. Webjorn, and P. A. Thomas, Journal of Applied Crystallography **29**(3), 279 (1996).
[9] A. A. Anikiev, L. G. Reznik, B. S. Umarov, and J. F. Scott, Ferroelectrics Letters **3**, 89 (1985).
[10] L. G. Reznik, A. A. Anikiev, B. S. Umarov, and J. F. Scott, Ferroelectrics **64**, 215 (1985).
[11] A. M. Prokhorov and Y. S. Kuz'minov, *Physics and Chemistry of Crystalline Lithium Niobate* (Adam Hilger, New York, 1990), p. 237.
[12] M. N. Palatnikov and N. V. Sidorov, "Some fundamental points of technology of lithium niobate and lithium tantalite single crystals," In *Oxide electronics and functional properties of transition metal oxides* (NOVA Science Publishers, USA, 2014), pp. 31–168.
[13] A. A. Anikiev, N. V. Sidorov, and Y. A. Serebryakov, J. Applied Spectroscopy (Minsk) **56**, 670 (1992).
[14] N. V. Sidorov, A. A. Yanichev, M. N. Palatnikov, and A. A. Gabain, Optics and Spectroscopy **116**, 281 (2014).
[15] N. V. Sidorov and M. N. Palatnikov, Optics and Spectroscopy **121**, 842 (2016).
[16] S. L. Chaplot and R. K. Rao, J. Phys. C: Solid State Phys. **13**, 747 (1980).
[17] K. Parlinsky, Z. Q. Li, and Y. Kawazoe, Phys. Rev. B **61**, 272 (2000).
[18] V. Caciuc, A. V. Postnikov, and G. Borstel, Phys. Rev. B **61**, 8806 (2000).
[19] N. V. Surovtsev, V. K. Malinovskiĭ, A. M. Pugachev, and A. P. Shebanin, Physics of the Solid State **45**, 534 (2003).
[20] N. V. Sidorov, A. A. Kruk, A. A. Yanichev, M. N. Palatnikov, and B. N. Mavrin, Optics and Spectroscopy **117**, 560 (2014).
[21] D. Phelan, X. Long, Y. Xie, Z.-G. Ye, A. M. Glazer, H. Yokota, P. A. Thomas, and P. M. Gehring, Phys. Rev. Lett. **105**, 207601 (2010).
[22] N. Zhang, H. Yokota, A. M. Glazer, Z. Ren, D. A. Keen, D. S. Keeble, P. A. Thomas, and Z.-G. Ye, Nature Communications **5**, 5231 (2014).
[23] M. A. Krivoglaz, *Theory of scattering of X-rays and thermal neutrons in nonideal crystals* (Nauka, Moscow, 1967), p. 336.
[24] J. Jackle, In *Amorphous Solids: Low-Temperature Properties*, Ed. W. A. Phillips (Springer, Berlin, 1981), p. 278.